



Specific Detection of Short-Chain Alcohols, with the Development of an Enzyme-Coated Microcantilever-Based Biosensor

Alexandre Margarido¹ · Livia Regina Manzine² · Fernando M. Araujo-Moreira^{3,4}  · Renato V. Gonçalves⁵  · Paulo Sergio de Paula Herrmann⁶ 

Received: 15 November 2021 / Accepted: 7 April 2022
© The Author(s) under exclusive licence to Sociedade Brasileira de Física 2022

Abstract

This work describes the development and evaluation of a biosensor designed for enzymatic detection of short-chain alcohols, using an X-ray photoelectron spectroscopy (XPS) and atomic force microscopy (AFM). The biorecognition element, alcohol dehydrogenase, was immobilized on self-assembled monolayers deposited on top of silicon nitride microcantilevers. Biosensor assays provided detection of short-chain alcohols and evaluation of the influence of a biological element immobilization on the analytical performance of the device. The self-assembly process was performed by surface activation using 3-aminopropyltriethoxysilane, followed by glutaraldehyde and biomolecule binding. XPS and AFM were used to verify surface oxidation and reagent binding. The biosensor showed a response time shorter than 1 s, a total renovation of the bioactive layer after 10 min, a sensibility from 0.03 to 1.2 mL/L, and a lifetime of 22 days. Its selectivity was analyzed through exposure to pure and mixed volatile solvents. Sensor sensibility was higher in the presence of short-chain alcohols family (methanol, ethanol, and propanol) ranging from 0.45 to 0.85 kHz and practically null involving other polar or nonpolar solvents. The biosensor showed less susceptibility to humidity and temperature variations, presenting a high-quality factor, a faster response time, selectivity, sensitivity, and durability.

Keywords Biosensor · Gas detector · Alcohol dehydrogenase · Short-chain alcohols · XPS · Microcantilever

1 Introduction

Alcohols are essential compounds in medicine, biotechnology, and mainly in the food industry, in which some procedures may involve fermentation and distillation. However,

in some cases, the volatilized concentration of alcohols—besides being highly flammable—can reach toxic levels, causing inflammation of the nasal and conjunctiva mucous membrane, skin irritation, and poisoning. Given these circumstances, monitoring the volatilized alcohol concentration in the air is essential [1–3]. In nature, the detection of methanol can signal plant immunity, with potential application in plant phenotyping [4].

A susceptible sensor requires the detection of small quantities—in the ppm range—of volatile organic compounds (VOC) in a gaseous medium. In this context, the development of microcantilever (μC)-based biosensors has been an efficient solution [5, 6]. Microcantilevers are mechanical probes with a particular format used to measure small forces, and different probes are employed for investigations with atomic force microscopes (AFM) [7]. Initial applications of a microcantilever as a sensor was a mass-sensitive balance, which acted as a microresonator, reaching resolutions in the order of picograms and allowing the detection of individual virus particles [8]. Microcantilevers with a high Q factor—in the order of 10,000—and high-frequency operations—around 1.5 MHz—allow a resolution

✉ Paulo Sergio de Paula Herrmann
paulo.herrmann@embrapa.br

¹ São Carlos, SP, Brazil

² Molecular Biotechnology Group, São Carlos Physics Institute, University of São Paulo, São Carlos, SP 13566-590, Brazil

³ Department of Physics, Federal University of São Carlos, São Carlos, SP 13565-905, Brazil

⁴ Graduate Program in Biotechnology, Department of Biotechnology, Federal University of São Carlos, São Carlos, SP 13565-905, Brazil

⁵ São Carlos Institute of Physics, University of São Paulo, São Carlos, São Paulo 13560-970, Brazil

⁶ National Nanotechnology Laboratory for Agribusiness, Embrapa Instrumentation, P.O. Box 741, São Carlos, SP 13560-970, Brazil

of theoretical mass of about 20 ag/Hz [9]. Usually, sensors translate the change in a physical property into measurable electrical signals; however, in this study, the AFM was used to examine the mechanical response of a μC . The immobilization of biomolecules, such as enzymes, in a sensor, promotes the affinity and high selectivity of catalytically active proteins high selectivity, to detection of a specific target and studies applying alcohol dehydrogenase enzyme immobilization have been reported for detection of alcohols using amperometric [1, 10, 11] and voltammetric sensors [12, 13]. The enzymatic biosensors offer a combination of performance and analytical features not available in other bioanalytical systems [14]. In the functionalization, the microcantilever can be coated on either side or just one side with a sensitive layer. They are making it possible to detect the mass variation in the set by changes in the resonant frequency. This reading method is known as a dynamic mode. The microcantilever is only coated on one side in the static mode and suffers a twist when exposed to an analyte. This twist is caused by interactions between the sensor and the surface layer. This variation of the technique is commonly used in liquid mediums [15].

The principle of operation of a cantilever sensor is based on the adsorption of analytes at the surface of the cantilever (coated with a sensing layer), which usually leads to an induced surface stress and an increase of the apparent mass of the cantilever [16]. The change in mass leads to deflection of the cantilever in the Z direction.

Treating the rectangular cantilever as a vibrating spring-mass system, its resonance frequency (f_{res} (Hz)) can be calculated as follows:

$$f_{\text{res}} = \frac{1}{2\pi} * \sqrt{\frac{k}{m}} \quad (1)$$

where k is the spring constant ($\text{N}\cdot\text{m}^{-1}$) and m the mass (g).

The mass of a cantilever can be expressed as $m = \rho \cdot h \cdot l \cdot w$, where ρ is the density ($\text{g}\cdot\text{m}^{-3}$) of the material, h its thickness (m), w its width (m), and l the length (m).

1.1 Microcantilever Surface Activation

The chemical modification or activation of microcantilever surfaces for the attachment of biomolecules is commonly performed using reagents such as 3-aminopropyltriethoxysilane (APTES) and alkanethiols, such as 11-amino-1-undecanethiol hydrochloride (THIOL) [16–18]. The surface activation using APTES can be performed directly on silicon, gold, and other materials through solution vaporization or immersion. In this process, the formation of silane compounds in self-assembled monolayers (SAMs) occurs by connecting silanol

groups (Si–OH) arranged on the surface of the oxidized microcantilever with active silanol groups in APTES. The formation of silanol groups in APTES is derived from a hydrolysis process of ethoxy terminal groups in the presence of organic solvents. Thus, the NH_2 end of APTES remains free, allowing adhesion of molecules through biocompatibility, charge, hydrophobicity, or hydrophilicity. The functionalized amino-silane can form covalent bonds through its amino group with other substances, such as glutaraldehyde (GLD)-mediated reaction or carboxyl groups [1-ethyl-3-(3-dimethyl aminopropyl) carbodiimide] (EDC) mediated by crosslinking of biomolecules [19].

The formation of multiple layers can occur when APTES molecules are physically adsorbed to each other on an already activated area. The APTES activation multiple layers was found in an air-dried environment formed one or two siloxane bonds on the surface. In comparison, the cured to heat activation (100 to 200 °C) tends to form three siloxane bonds on the surface, helping to remove solvent excess [20].

1.2 Immobilization of Biomolecules on Microcantilever Surfaces

Immobilization of biomolecules on microcantilever surfaces can be seen as closely related to the immobilization methods used to fabricate electrodes; these procedures are gathered under the generic term “chemically modified devices” [17]. The binding of biomolecules by the SAM process is desirable as it provides a stable immobilization [21], and it occurs when functional groups of organic materials (such as -OH, -NH₂, -COOH and -SH), which are not essential to the catalytic activity of the enzyme, bind to available APTES groups. To achieve that, knowledge of the enzyme structure is paramount [17]. The alcohol dehydrogenases used in this experiment contain 374 amino acid residues per chain and 95 lysine residues available on the enzyme’s surface, enabling multiple bonds [17]. Groups of E carbon (EC) from lysine residues of biomolecules are commonly used as binding means, but linkages with tyrosine, tryptophan, phenylalanine, and cysteine amino acids may also occur [22, 23]. For an appropriate result, the biomolecule immobilization process involves three main steps: (i) surface activation, (ii) biomolecule coupling, and (iii) removal of weakly bound biomolecules [17]. The enzyme used in this study as a biorecognition element allowed the binding of specific analytes transformed into by-products or simply left the biomolecule after a short time, renewing the biosensor for the next reading process [18]. This paper presents a specific enzymatic biosensor that uses a signal transduction based on mechanical displacement, which differs from commonly commercially available voltammetric and resistive sensors.

2 Materials and Methods

2.1 Reagents

The water used for solutions preparation was purified at 18 M Ω .cm resistivity by the Milli-Q system (Millipore Inc.).

All chemicals and buffer components were used as received. The solvent toluene, ACS grade, 99.5%, was provided by J. T. Baker. All the other reagents were purchased from Sigma-Aldrich. These products were 3-aminopropyltriethoxysilane (APTES) 99%, 0.946 g/mL at 25 °C, triethylamine \geq 99%, 101.1 g/mol, glutaraldehyde (GLD), solution grade I, 25% in H₂O, and alcohol dehydrogenase from *Saccharomyces cerevisiae* (yeast), lyophilized powder, with \geq 300 units/mg of protein, MW 141–151 kDa (Sigma Aldrich A7011).

The standard assay was performed according to the Sigma Aldrich protocol (cod. A7011) to evaluate the enzymatic activity. The reaction can be followed by the transformation of ethanol in the presence of β -NAD to acetaldehyde and β -NADH, where one unit of the enzyme

is responsible for the conversion of 1.0 μ mole of ethanol to acetaldehyde per minute at pH 8.8 at 25 °C. A Shimadzu UV-1650PC UV–Visible spectrophotometer in the UV region (340 nm) was used to obtain the curve of absorbance versus time, related to the amount of β -NADH that is released in the conversion reaction.

2.2 Microcantilevers

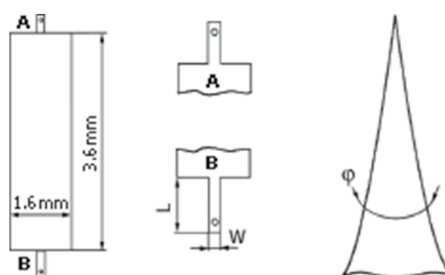
Silicon microcantilevers used were HA_NC model (NT-MDT) with stems at ends, being (A) the shortest and (B) the longest, as Table 1 shows.

2.3 Instrumentation

The frequency response of the microcantilevers during excitation was measured using a Veeco Dimension V AFM. The laser was focused on the apex of the cantilever and reflected in a position-sensitive detector. In dynamic mode, an internal

Table 1 Physical characteristics of the microcantilevers used in this study and the image of shape of polysilicon lever, monocrystal silicon tip (NT-MDT, HA_NC model)

Characteristic	A	B	Typical dispersion
Length, L (μ m)	94	124	\pm 2
Width, W (μ m)	34	34	\pm 3
Thickness, H (μ m)	1.85	1.85	\pm 0.15
Force constant (N/m)	12	3.5	\pm 20%
Resonant frequency (kHz)	235	140	\pm 10%



NT-MDT (HA-NC) Polysilicon lever, Monocrystal silicon tip

Table 3 Percentage of chemical elements in each sample measured by XPS

Sample	O 1s (%)	C 1s (%)	Si 1s (%)	N 1s (%)	I (%)
1	39.45	28.43	32.12	-	-
2	35.67	27.65	34.44	1.75	0.5

spectra were corrected in relation to the binding energy of the carbon peak set at 284.8 eV (C 1s). Data was processed using the CasaXPS software (Casa Software Ltd., UK).

2.6 Biosensor Selectivity

To investigate the selectivity of this biosensor, volatile organic compounds were used (Table 3) and applied at the same concentration, calculated as the ratio of the number of VOC molecules to the amount of air molecules available in a 2.0 L reservoir used in the experiment [18].

Using Eq. (2) the ratio of the amount of VOC molecules to the quantity of air molecules in a reservoir of known capacity, the VOC concentration (Y_i) in ppm was estimated:

$$Y_i(\text{ppm}) = \frac{V_{\text{voc}} * \rho(\text{voc})}{MW(\text{voc})} * \frac{R * T}{P * V(\text{chamber})} \quad (2)$$

where the universal gas constant (R) = 0.0821 (L*atm*K-1*mol-1), temperature (T) (Kelvin (°K) = (°C) + 273.16), local atmospheric pressure (P) (0.9088 atm), and volume of the chamber (V_{chamber}) = 2.0 (L).

3 Results and Discussion

3.1 Characterization of the Activated Surface by X-ray Photoelectron Spectroscopy

Two samples were prepared for XPS analysis: a microcantilever of Si treated with piranha solution (70% H₂SO₄ + 30% H₂O₂) for 5 min and washed with mil-li-Q (sample 1) and a microcantilever of Si treated with piranha solution (70% H₂SO₄ + 30% H₂O₂) for 5 min, washed with milli-Q and covered by a layer originated from the vaporization of 40 μL of APTES and 40 μL of triethylamine for 1 h in a desiccator purged with nitrogen (sample 2—steaming method). The composition of each element measured by XPS is described in Table 4.

Figure 2 shows the complete XPS spectrum for each microcantilever. The identified peaks offer the chemical elements and the electronic configurations in the samples. Both specimens presented Si 2p and Si 2s on the surface and a peak near 285 eV associated with C 1s. The carbon present in the samples may be due to functionalization with APTES or exposure of the samples to air [26]. It is well known from the literature that exposure of samples to the environmental atmosphere can lead to the formation of a thin layer (~2 nm) of carbon-rich material on the surface, known as adventitious carbon, easily detected by XPS [26]. The spectrum in Fig. 2(A) shows an intense peak of O 1s that can be assigned to the passivation of a SiO₂ oxide layer on the surface caused by piranha solution. A strong signal of O 1s and no signal of N 1s was observed on the survey

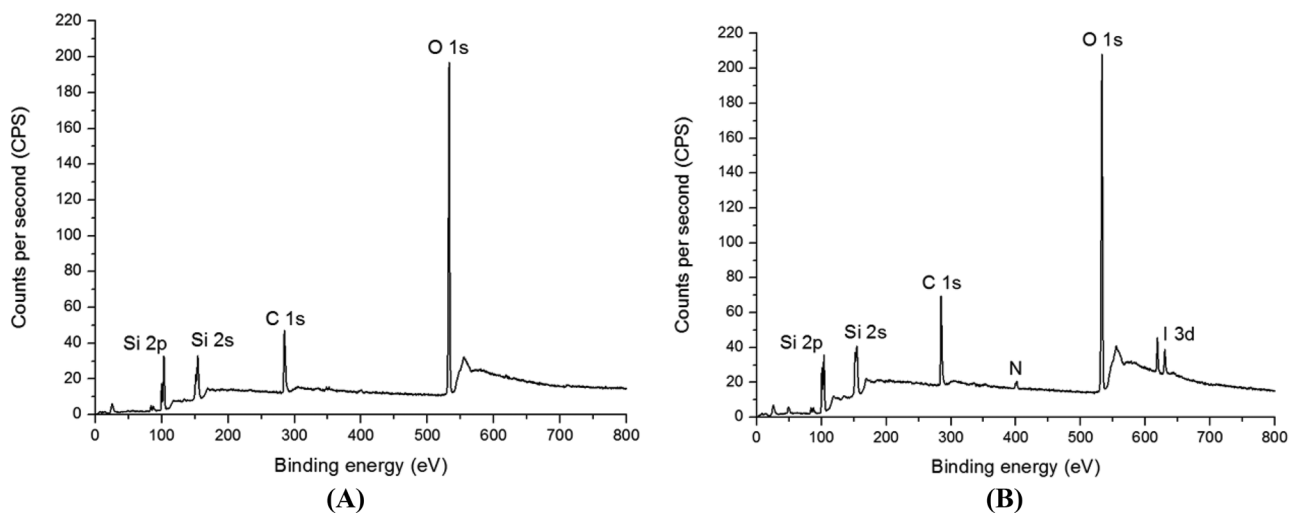


Fig. 2 XPS spectra for Si microcantilevers (A) after 5 min in piranha solution (sample 1) and (B) after activation by vapor treatment with APTES and triethylamine for 1 h (sample 2) [18]

spectrum of XPS for sample 1. This result confirms a thick layer of SiO_2 on the surface of the μC due to treatment with piranha solution (oxidation). For sample 2, the presence of N 1 *s* at 399.5 eV can be seen, suggesting that the sample was activated with APTES. A strong peak of N 1 *s* was expected in this sample because of the material the μC was made from; nevertheless, treatment with piranha solution led to the formation of a layer of SiO_2 on the surface of the substrates, which the intense peak of O 1 *s* can confirm.

In addition to nitrogen, carbon is another abundant element in APTES ($\text{C}_9\text{H}_{23}\text{NO}_3\text{Si}$) and can be an indicator in the samples. However, the carbon present in these samples may have two sources, adventitious C 1 *s*, from atmospheric air and APTES. Because the samples were submitted to the same treatment with piranha solution and had the same exposure time to air, it is possible to assume that the concentration of adventitious C 1 *s* is the same in both samples. The results exhibited in Fig. 2 reveal that the XPS technique satisfactorily indicated the success of surface activation of microcantilevers, confirming the presence of APTES N 1 *s* element.

Figure 3 display the high-resolution spectra of Si 2*p*, C 1 *s*, and N 1 *s* for the Si microcantilevers after activation by vapor treatment with APTES and triethylamine. The peak centered around 102.6 eV can be assigned to SiO_2 [27], while the peak at 99 eV has been reported for the Si–N species (Fig. 3(A)) [28]. The presence of silicon oxide is expected due to the cleaning of the microcantilever substrate

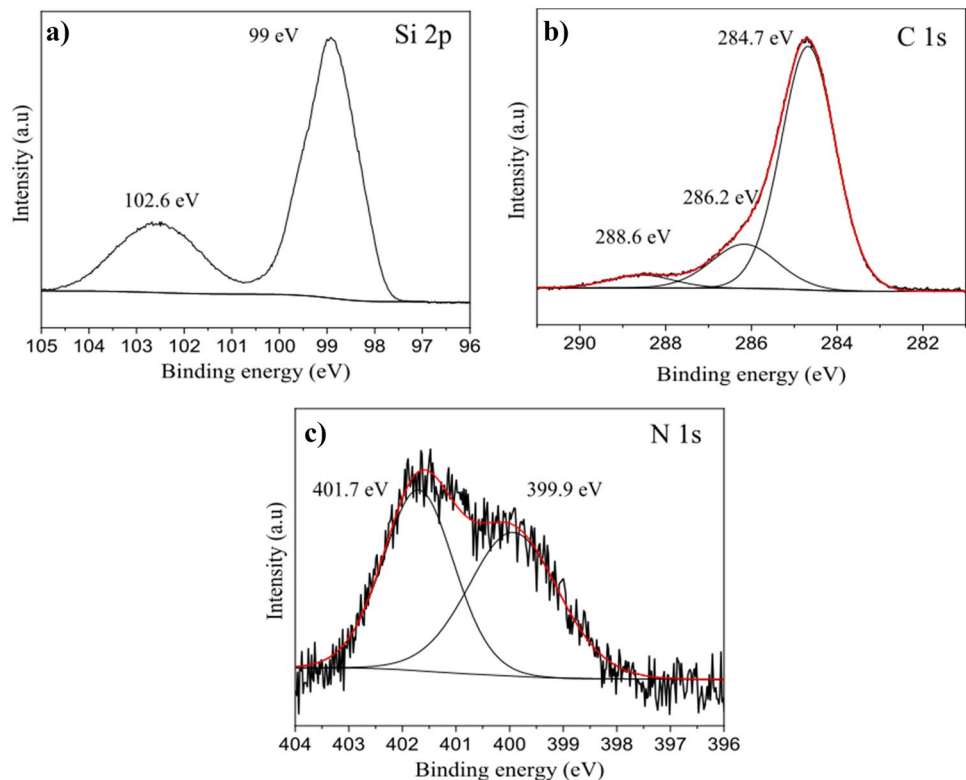
with piranha solution that is a strong oxidizing agent [26]. Indeed, the peak observed at ~ 530 eV with the highest intensity (Fig. 2(B)) is attributed to the O 1 *s*, which indicates that the substrate has a silicon oxide layer on the surface. The high-resolution XPS peak for C 1 *s* was adjusted with three components centered at 288.6, 286.2, and 284.7 eV, respectively (Fig. 3(B)). The binding energy at 286.3 eV is assigned to C–N groups, suggesting that the microcantilever was functionalized with APTES [26, 29]. Other two peaks at 288.5 and 284.7 eV correspond to O–C=O and C–C groups, respectively. The peak centered at 284.7 eV is well known from literature for adventitious carbon due to the exposure of samples to the environmental atmosphere [27].

The high-resolution XPS spectra of N 1 *s*, showing in Fig. 3(C), were adjusted with two components centered at 401.7 and 399.9 eV, assigned to amine groups from APTES [30, 31]. The XPS results confirming the presence of APTES on the surface of the microcantilever substrate. The composition of each element measured by XPS is described in Table 4.

3.2 Microcantilever Functionalization

Figure 4 highlights the results of μC activation with APTES steaming technique followed by functionalization process by glutaraldehyde and alcohol dehydrogenase enzyme. The change in the resonant frequency (Fig. 4(A)) and quality factor *Q* (Fig. 4(B)) for each step of the construction of the

Fig. 3 High-resolution XPS spectra for Si microcantilevers **a)** after activation by vapor treatment with APTES and triethylamine for 1 h (sample 2). The **b)** XPS peak for C 1 *s* and **c)** XPS spectra of N 1 *s* [18]



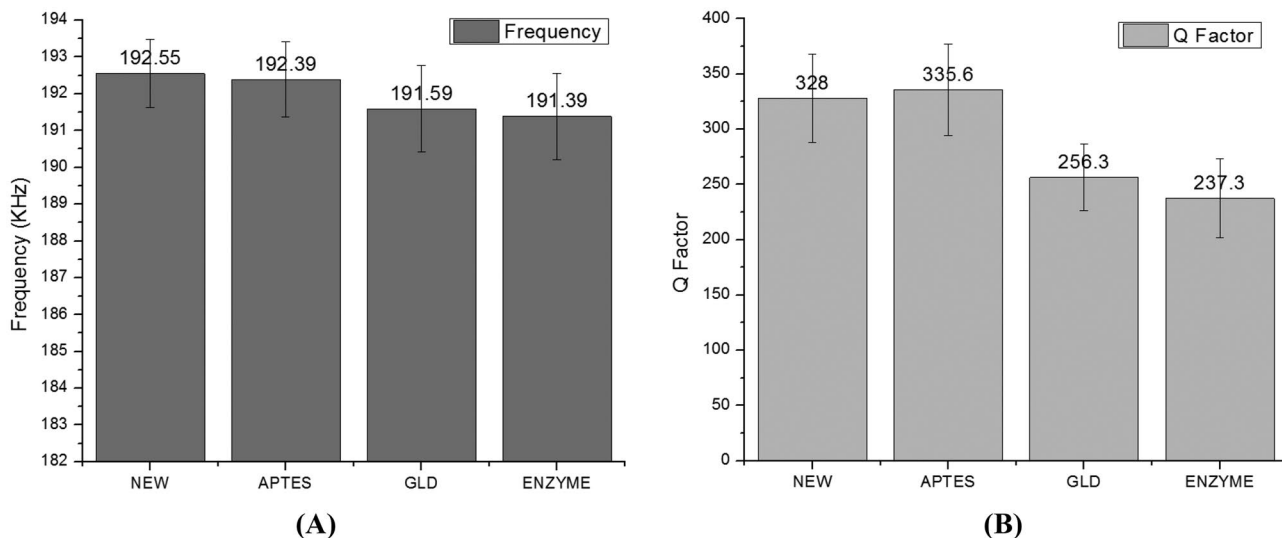


Fig. 4 Variation of resonant frequency (A) and Q factor (B) for each step of the functionalization process

biosensor is shown. The observed decrease in the resonant frequency indicates the increase of mass on the surface of the microcantilever stem [18], with the confirmation of the subsequent molecular bindings of the functionalization procedure.

Other surface activation techniques have also been tested, such as immersion in APTES and THIOL solutions. The activation by immersion in APTES is hard to be controlled and usually results in the formation of undesirable multiple layers. For activation with THIOL, a thin gold layer deposition on the substrate is necessary, which modifies the physical characteristics of the microcantilever and is related to various drawbacks, such as the ease of absorbing organic compounds [18]. Therefore, these techniques were not used in this work due to the limitations described herein.

3.3 Characterization of Functionalized Surface with Alcohol Dehydrogenase

The calculation of the functional layer thickness was performed through AFM in the contact mode. The thickness measurement was used to assess thin film formation on the substrate with a topography image and to obtain quantitative information of the absorption. A sharp metal blade, with hardness lower than the substrates, was used to avoid damaging his surface. The functionalized surface was scratched until the silicon substrate from the AFM probe (substrate, cantilever, and probe) was reached, removing only part of the functional layer. From the cross-section (Fig. 5(B)), it is noted that the region where the functionalization remained unchanged (interface between the two surfaces) showed an accumulation of material (the region between 2.4 and 3.6 μm), to the blade pulling part of the functional layer

when making the scratch. The image was obtained on the forming step, allowing to estimate the layer's thickness. Figure 5(A) shows the groove in a functionalized μC whose coverage resembled a monolayer. The thickness added by each functionalization step can be estimated based on the information available in the literature. Activation with APTES and layers of glutaraldehyde and alcohol dehydrogenase contribute to thicknesses of 0.70, 0.30, and 9.05 nm, respectively, which results in a total thickness of 9.79 nm. Experimentally, the average thickness was 14.68 ± 1.19 nm (Fig. 5(B)). This variation in thickness is because both APTES and glutaraldehyde can form multiple layers; the presence of geometric imperfections or residues on the surface of the microcantilever may also explain this difference.

3.4 Biosensor Response to Target Analyte

A notable variation of surface tension on the functionalized stem of the microcantilever freely oscillating in a chamber saturated with volatile alcohols was noticed when the biosensor was exposed to a significant concentration of ethanol at ambient conditions (25 $^{\circ}\text{C}$, 1 atm, relative humidity of 50%). This event is evidenced both by its bending when only one face is functionalized and by the significant increase in the resonant frequency if both sides are functionalized.

The response of the resonant frequency of the biosensor to 10 μL of pure ethanol in both sides of the functionalized μC in three consecutive tests of 20 min each is depicted in Fig. 6. The variations in the relaxation time of the biosensor may be adaptations of the biomolecule on the surface of the microcantilever or occupation of enzyme active sites; however, the maximum surface tension remained the same during the three tests. It was also noted that the adsorption

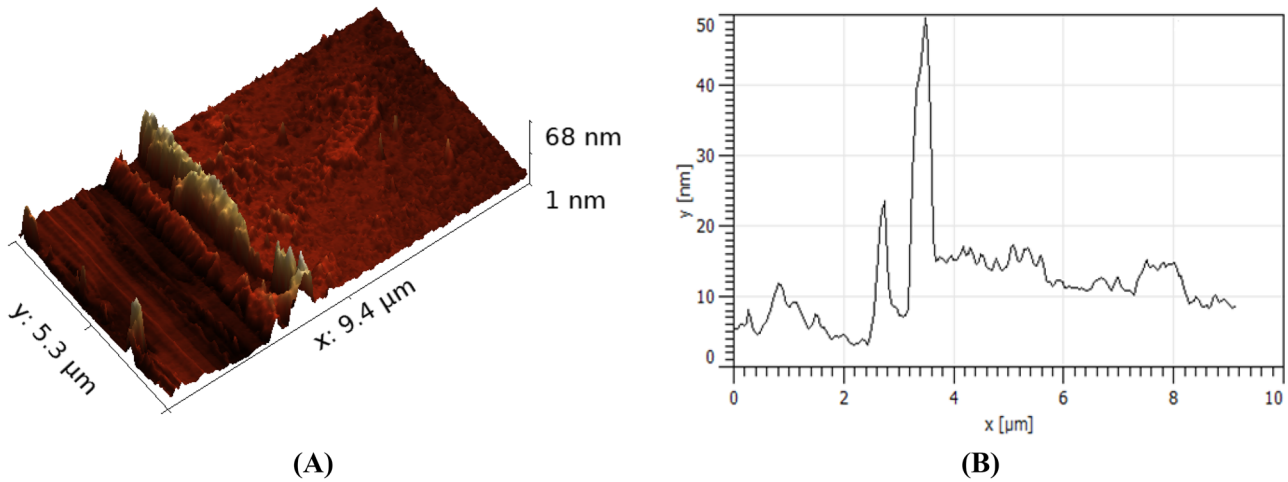


Fig. 5 Microcantilever activation with APTES steaming technique. Average thickness around 14.68 ± 1.19 nm in the region between 4 and 9 μm and between 0 and 5 μm in the region where the groove

for removal of material was made. (A) A 3D view and (B) an aleatory profile of the topography with the average thickness of ten cross-sections [18]

phase, associated with a decrease in resonant frequency, became shorter throughout the experiment, possibly because ethanol vapor expels the humidity in the biosensor, thus changing the resonant frequency in each assay.

Figure 7 exhibits and highlights parts of the frequency curve associated with significant immobilization events for comparison. The cantilever is oscillating freely in a chamber saturated with volatile alcohols. The interaction of ethanol vapor with the bare μC did not influence the resonant frequency response.

It was observed that a higher concentration of ethanol caused a significant increase in the resonant frequency due to the increase in surface tension. It is believed that the increase in surface tension is related to a conformational change of the ethanol-bound enzyme when compared to the unbound enzyme. This fact was also confirmed experimentally by the decrease in roughness and increase in thickness. As the enzyme cofactor is not present in this condition, it is assumed that the active site only binds to the substrate and releases it because of air drag, without leading to the

Fig. 6 Resonant frequency response of the microcantilever in three consecutive assays using 10 μL of 99.9% ethanol deposited on a glass slide at 5 mm from the biosensor. Data were normalized (kHz/kHz) for comparison of the response profiles

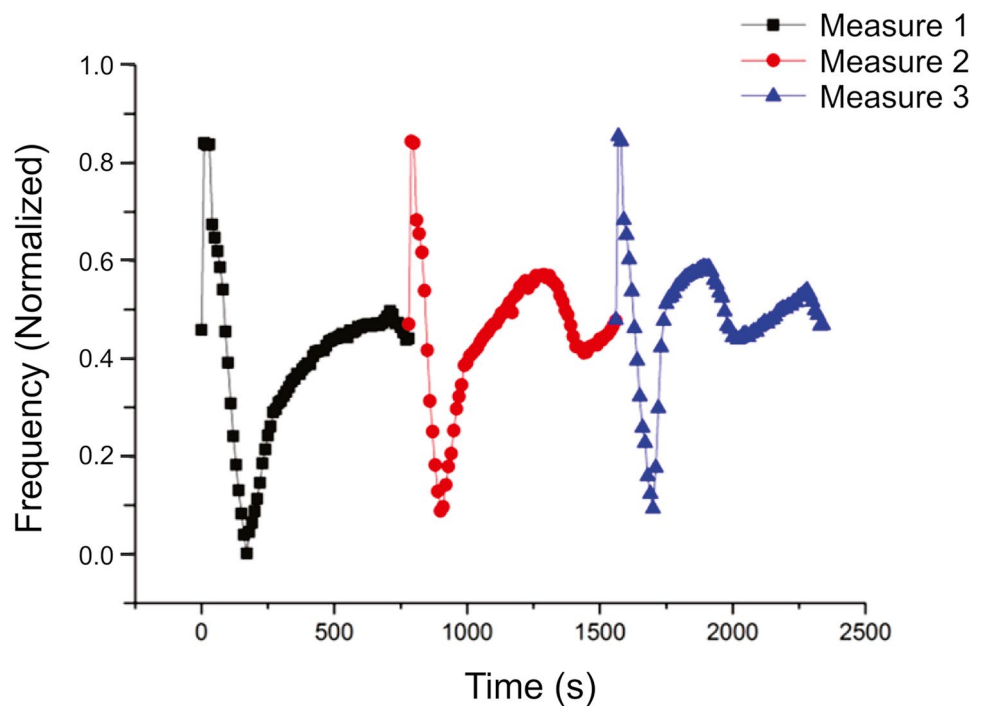
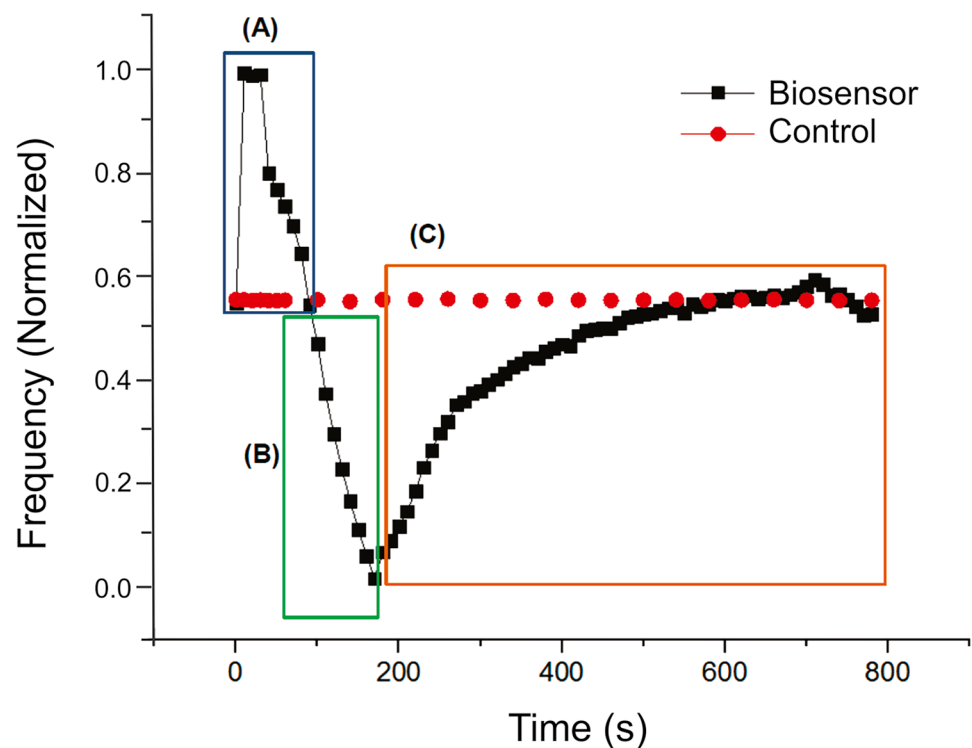


Fig. 7 Comparison of the response of a bare (control) (●) and a functionalized (biosensor) (■) μC exposed to $10\ \mu\text{L}$ of ethanol vapor; region (A) shows the influence of the surface tension, part (B) depicts adsorption, with a decrease of the resonant frequency, and (C) corresponds to the biosensor recovery



formation of the product. When ethanol binds to the active sites, it causes the expulsion of the water molecules present, thus altering the resonance frequency due to mass variation. Evaporation of ethanol provides a high concentration of this molecule in the first contact, which causes the surface tension of the biosensor to increase significantly and very quickly. As the ethanol concentration decreases, the surface tension decreases to the point where it is no longer observed. Subsequently, the change in resonance frequency decreases due to mass adsorption until the ethanol vapor is completely discharged, a process that takes about 5 min. Regarding adsorption, the decrease in the resonant frequency (phase B in Fig. 7) may be related to the fact that the ethanol vapor expels the moisture present in the biosensor, thus altering the resonant frequency. The biosensor recovery time was verified, with the response monitored for the next 15 min. Figure 8 shows the changes in the resonant frequency of the biosensor without the target analyte in the first 10 min of operation, with an acquisition rate of one reading per minute. At time $t=0$, a slide was inserted with $10\ \mu\text{L}$ of ethanol at 5 mm from the biosensor under ambient conditions.

To determine the effect of ethanol concentration on the resonant frequency, a 2-l closed circulatory system was developed containing a special cell to seal the μC support to minimize any interference in the system. Figure 9 shows that for ethanol concentrations above $0.3\ \text{mL/L}$ a surface tension was observed, causing an increase of resonant frequency much more significant than the increase of mass adsorbed on the surface. At concentrations above $0.6\ \text{mL/L}$,

the exponential growth of the resonant frequency occurred and stabilized upon saturation of the biosensor. In the interval between 0.2 and $0.4\ \text{mL/L}$, there is a balance between adsorption and surface tension in which there is no significant variation of the resonant frequency.

This transition makes the biosensor less sensitive to identify a specific concentration, but it can still be used to determine a range of concentrations.

Figure 9 reveals that up until the ethanol concentration of $0.03\ \text{mL/L}$, the biosensor suffered a reduction in resonance frequency; the saturation point, related to the highest resonant frequency, was registered at a concentration of $1.2\ \text{mL/L}$. This data shows a high selectivity and a wide short-chain alcohols detection range of this enzymatic biosensor which can detect ethanol concentrations from 0.03 – $1.2\ \text{mL/L}$. Commercial devices, even with a detection range of 0.0011 – $0.21\ \text{mL/L}$ (HANWEI ELECTRONICS CO. MQ-3 GAS SENSOR) show different resistance values to various kinds and concentrations of gases, which makes these sensors unattractive to selectivity and specificity parameters. Furthermore, the response of commercial sensors depends on the environment humidity, a correlation not observed for the biosensor developed in this study.

The experiment with three functionalized biosensors (Fig. 9) also shows that these devices, even being made from the same model of μC , are not identical, as they present small variations in all dimensions, resulting in different sensitivities (variation in resonant frequency), different numbers of immobilized biomolecules, and other subtle

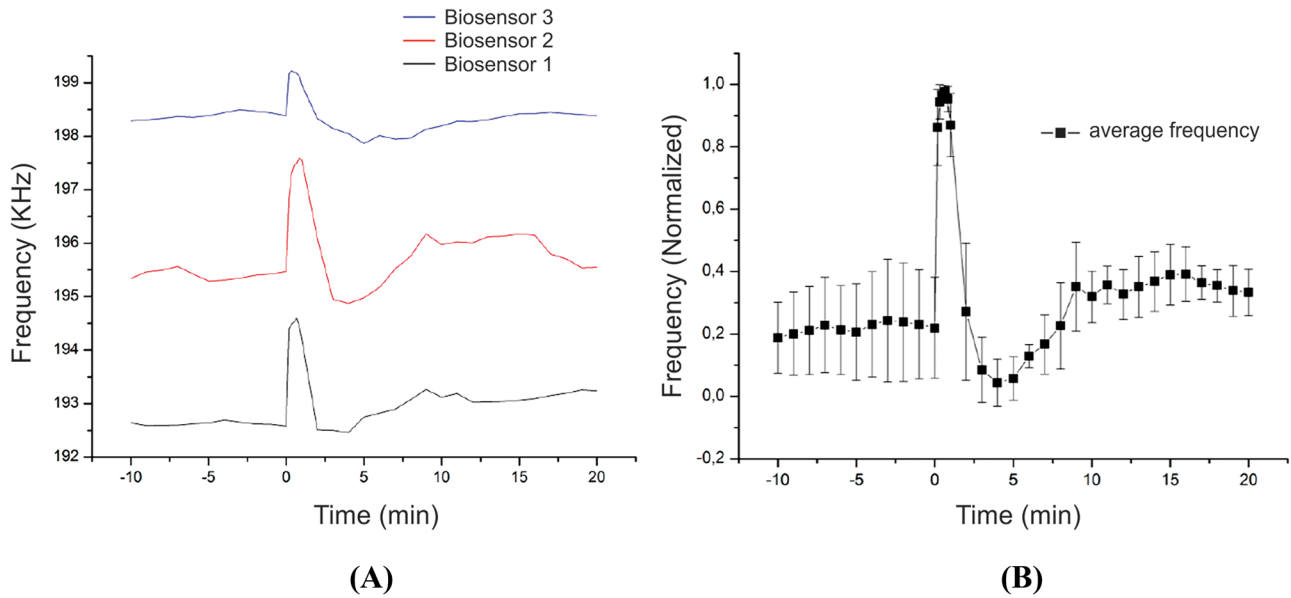


Fig. 8 Three different biosensors with steam powered APTES. The thin and uniform layer makes the most efficient biosensors and reduces the difference between the behaviors

discrepancies; however, the biosensors detection behaviors are considerably similar when exposed to the target analyte.

To verify the selectivity of the biosensor, tests were carried out with different VOCs as analytes, in the same molar concentration of the 10- μ L ethanol sample. These results are shown in Figs. 10 and 11.

In the graph in Fig. 10, CONTROL represents the AFM response with the biosensor in ambient conditions without any analyte. The biosensor undergoes a slight variation in the resonant frequency over the observed period, forming a sine wave that can be observed in Fig. 7 between 0 and 10 min. Water molecules may occupy the interior of the active sites of the enzyme, causing a variation in

resonant frequency due to changes in the mass of the microcantilever.

The selectivity of the biosensor was analyzed to different VOCs at the same time and conditions (Fig. 11). When the biosensor was exposed to the VOCs mix without ethanol, a small decrease in the resonant frequency (adsorption) was observed at first contact; however, after 2 min, the resonant frequency resumed its original value. The shape of the biosensor recovery curve shown in Fig. 6 was also observed in the vapor assay with the VOC mixture (Fig. 11(B) and (C)).

The selectivity of the biosensor was tested under the following conditions: 3 consecutive assays followed by 20 min of exposure to 10 μ L of ethanol (Fig. 11(B)); 3 consecutive assays followed by 20 min of exposure to a 61.7- μ L mixture

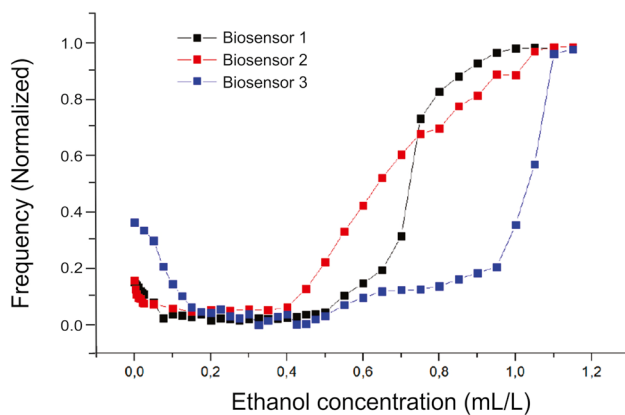


Fig. 9 Resonant frequency variation as a function of ethanol concentration from 0 to 1.2 mL/L in an enclosed circulatory system for three monolayer functionalized biosensors

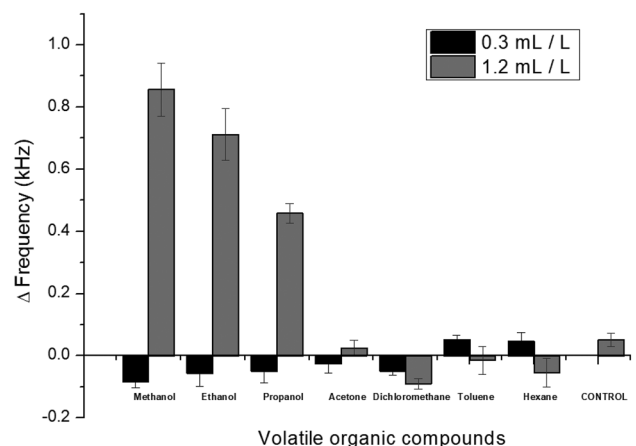


Fig. 10 Selectivity test with different VOCs at concentration range from 0 to 0.3 mL/L (black bars) and 0.4 to 1.2 mL/L (gray bars)

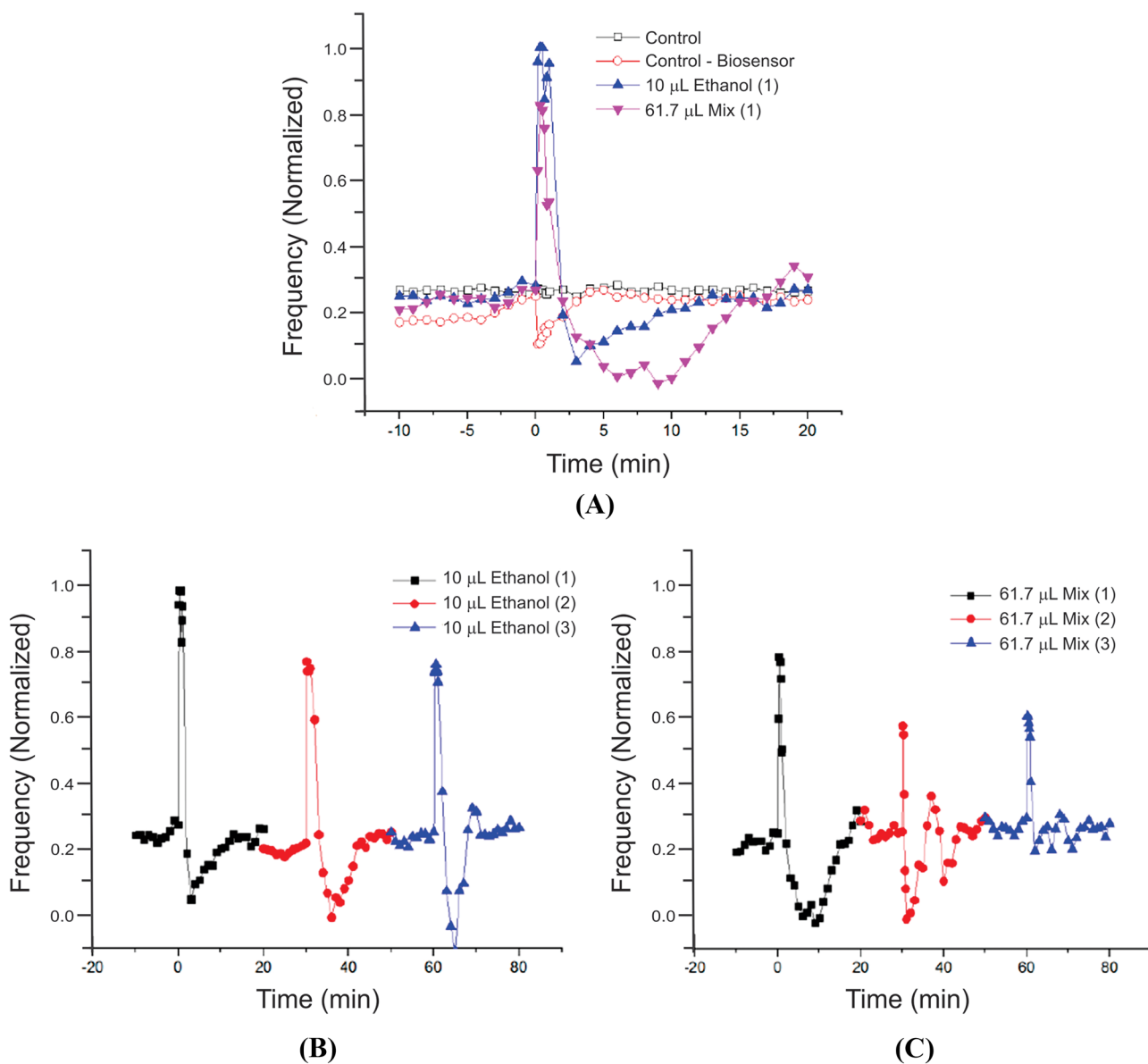


Fig. 11 Resonant frequencies under distinct conditions are compared: (A) control (\square) shows the response of a new μC without functionalization to the vapor of a mixture with ethanol, hexane, dichloro-methane, and toluene; control—biosensor (\circ) corresponds to a functionalized μC exposed to the vapor of a mixture with dichloromethane, hexane, and toluene; 10 μL ethanol (1) (\blacktriangle) exhibits the result for a function-

alized μC exposed to 10 μL of ethanol and 61.7 μL mixture (1) (\blacksquare) displays the results of a functionalized μC exposed to the mixture with four VOCs. (B) Biosensor response in a sequence of three experiments (\blacksquare , \bullet , and \blacktriangle) with exposure to 10 μL of ethanol and (C) with exposure to 61.7 μL of the mixture with four VOCs

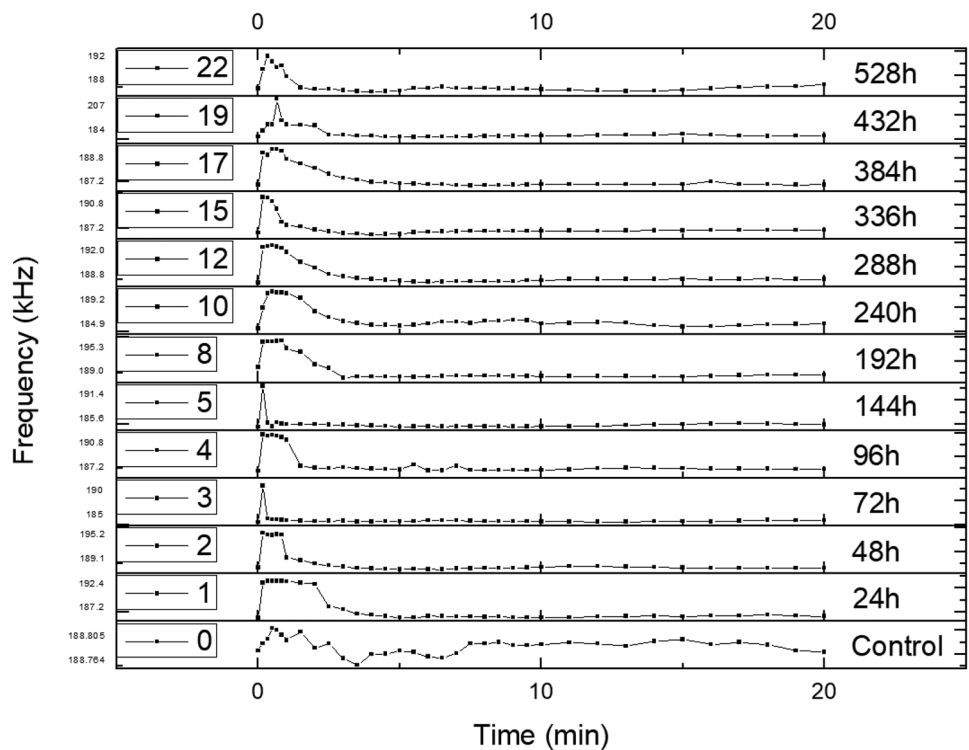
of VOCs (ethanol, hexane, dichloromethane, and toluene) containing 10 μL of ethanol (Fig. 11(B)). The control sample was tested for two different possibilities: biosensor exposed to the vapor of the mixture of three volatiles (dichloromethane, hexane, and toluene) and a new μC exposed to the steam of the combination of three volatiles (dichloromethane, hexane, and toluene) (Fig. 11), and compared with the biosensor assays with exposure to 10 μL of ethanol and 61.7 μL of the mixture of dichloromethane, hexane, toluene, and

ethanol. The total vaporization time for 10 μL of ethanol was around 5 min and for the sample with 61.7 μL of the mixture approximately 10 min.

A sensitivity test under ambient conditions evaluated the useful life of the biosensors. Devices were stored at 8.0 $^{\circ}\text{C}$ for 7 days prior to use and then used in daily tests for 22 days to determine their lifetime and sensitivity. Figure 12 exhibits the resonant frequency curve for some of these 22 days. At the end of the experiment, the biosensor remained sensitive;

Fig. 12 Biosensor lifetime.

After 22 days, the biosensor remained active, but showed an increase in the surface opacity, which prevented proper measurements with AFM. The variation, expressed in kHz (minimum and maximum frequency), corresponds to the sensitivity in 22 tests, carried out with 10 μL of ethanol vapor



however, increased opacity was observed, which hindered AFM experiments.

The present enzymatic biosensor can be used in a wide range of applications, such as environmental, manufacturing processes, and safety monitoring. Unlike the common affinity biosensors used for molecular imprinted polymers, oligonucleotides and antibodies, in this study, the enzyme–substrate interaction was successfully monitored and quantified using a microcantilever on dynamic mode. Besides, the use of a biological macromolecule for ethanol and others short-chain alcohols detection makes this biosensor highly selective and provides an important additional characteristic compared to commercial sensor, the specificity afforded by enzymes.

4 Conclusions

The functionalization of microcantilevers with alcohol dehydrogenase enzyme immobilized in self-assembled monolayers allowed the construction of a biosensor for selective detection of short-chain alcohols, at ambient conditions, even in the presence of a mixture of VOCs. The results obtained with the resonance frequency variation allowed us to observe the surface tension change: even when applying the coating with biomolecules and evidence of his immobilized activity. Images performed on the silicon substrate of the probe, using the contact mode of the atomic force microscope (AFM), and prepared according to the cantilever, allowed for the analysis and comparison of

the topography of the functionalized surface. The biosensor sensitivity is between 0.03 and 1.2 mL/L, and the device showed significant stability for 22 days. The biosensor surface was characterized through XPS and AFM techniques, which confirmed the formation of a self-assembled monolayer. XPS characterized the microcantilever surface activation process, showing that the activation by vaporization of reagents was successful. The sensitivity and selectivity of this enzymatic biosensor differ from that of other commercial sensors with considerable advantages. The device can operate in air or in an aqueous solution, allowing for the estimation of short-chain alcohols concentration. Repeatability tests revealed similar responses after 15 repetitions, with a half-life of around 432 h. This biosensor can also operate in almost any conditions of relative humidity, with optimum temperature around 25.0 ± 3.0 °C and pH 8.6. The biosensor can be stored at 8.0 °C for long periods without compromising the activity of the biomolecule.

Future work should be carried out to apply this new type of biosensor in practical situations, such as selective measurement of short-chain alcohols in the fermentation and distillation of food, wine, and volatiles of interest to plant phenotyping, such as methanol, for example.

Acknowledgements The authors would like to thank the National Council for Scientific and Technological Development (CNPq) (141267/2013-5) for its financial support and Embrapa Instrumentation for the infrastructure used to run the experiments. Dr. Rubens Bernardes Filho is a researcher from Embrapa Instrumentation for the image with AFM in contact mode, Professor Renato Vitalino

Gonçalves, the Crystal Growth and Ceramics Group (IFSC-USP)/ Center for Development of Ceramic Materials (CDFM—FAPESP process 2013/07296-2) for XPS measurements and Graduate Program in Biotechnology (PPGBiotec) at the Federal University of São Carlos.

Funding This work was financially supported by Embrapa Instrumentation, National Laboratory of Nanotechnology for Agribusiness (NLNanoAgr), project grant number 01.14.03.001.03.00 and the National Council for Scientific and Technological Development (CNPq) (141267/2013–5) for the scholarship.

References

- C.X. Cai, K.H. Xue, Y.M. Zhou, H. Yang, Amperometric biosensor for ethanol based on immobilization of alcohol dehydrogenase on a nickel hexacyanoferrate modified microband gold electrode. *Talanta* **44**(3), 339 (1997). [https://doi.org/10.1016/S0039-9140\(96\)020498](https://doi.org/10.1016/S0039-9140(96)020498)
- G. Ponce, J.C.C. Miranda, R. Maciel, R.R. de Andrade, M.R.M. Wolf, Icheap12: 12th International Conference on Chemical & Process Engineering, **43**, 319 (2015)
- A. Margarido, L.R. Manzini, F.M. Araujo-Moreira, R.V. Gonsalves, P.S.P. Herrmann, in Development of an enzyme-coated microcantilever-based biosensor for specific detection of short-chain alcohols. *Eng. Proc.* **6**, 75 (2021). <https://doi.org/10.3390/I3S2021Dresden-10175>
- T.V. Komarova, E.V. Sheshukova, Y.L. Dorokhov, Cell wall methanol as a signal in plant immunity. *Front. Plant Sci.* **5**, 101 (2014). <https://doi.org/10.3389/fpls.2014.00101>
- C. Steffens, F. Leite, C. Bueno, A. Manzoli, P.S.P. Herrmann, Atomic force microscopy as a tool applied to nano/biosensors. *Sensors* **12**(6), 8278 (2012). <https://doi.org/10.3390/s120608278>
- R. Manai, E. Scorsone, L. Rousseau, F. Ghassemi, M. Abreu, G. Lissorgues, N. Tremillon, H. Ginisty, J. Arnault, E. Tuccori, M. Bernabei, K. Cali, K. Persaud, P. Bergonzo, Grafting odorant binding proteins on diamond bio-MEMS. *Biosens. Bioelectron.* **60**, 311 (2014). <https://doi.org/10.1016/j.bios.2014.04.020>
- T.R. Albrecht, S. Akamine, T.E. Carver, C.F. Quate, Microfabrication of cantilever style for the atomic force microscope. *J. Vac. Sci. Technol. A* **8**(4), 3386 (1990). <https://doi.org/10.1116/1.576520>
- A. Gupta, D. Akin, R. Bashir, Single virus particle mass detection using microresonators with nanoscale thickness. *Appl. Phys. Lett.* **84**(11), 1976 (2004). <https://doi.org/10.1063/1.1667011>
- E. Finot, A. Passian, T. Thundat, Measurement of mechanical properties of cantilever shaped materials. *Sensors-Basel* **8**(5), 3497 (2008). <https://doi.org/10.3390/s8053497>
- S. Miyamoto, T. Murakami, A. Saito, J. Kimura, Development of an amperometric alcohol sensor based on immobilized alcohol dehydrogenase and entrapped NAD⁺. *Biosens. Bioelectron.* **6**(7), 563 (1991). [https://doi.org/10.1016/0956-5663\(91\)80020-X](https://doi.org/10.1016/0956-5663(91)80020-X)
- Ö. Çolak, Amperometric biosensing of ethanol-based on integration of alcohol dehydrogenase with a Pt/PPy--PVS/MB electrode. *Turk. J. Chem.* **39**(1), 84 (2015). <https://doi.org/10.3906/kim-1405-44>
- S. Alpat, A. Telefoncu, *Sensors* **10**(1), 748 (2010)
- Y. Liu, F. Yin, Y. Long, Z. Zhang, S. Yao, Study of the immobilization of alcohol dehydrogenase on Au-colloid modified gold electrode by piezoelectric quartz crystal sensor, cyclic voltammetry, and electrochemical impedance techniques. *J. Colloid Interface. Sci.* **258**(1), 75 (2003). [https://doi.org/10.1016/S0021-9797\(02\)00083-8](https://doi.org/10.1016/S0021-9797(02)00083-8)
- J. Halánek, Special issue information, "enzymatic biosensors". *Sensors* **13**(4), (2013). https://www.mdpi.com/journal/sensors/special_issues/enzymatic-biosensors?view=compact&listby=date#editors. Accessed 20 Oct 2021
- R. Berger, E. Delamarche, H.P. Lang, C. Gerber, J.K. Gimzewski, E. Meyer, H.J. Guntherodt, Surface stress in the self-assembly of alkanethiols on gold probed by a force microscopy technique. *Appl. Phys. a-Mater.* **66**, S55 (1998). <https://doi.org/10.1007/s003390051099>
- C. Steffens, F.L. Leite, C.C. Bueno, A. Manzoli, P.S.P. Herrmann, Atomic force microscopy as a tool applied to nano/biosensors. *Sensors* **12**, 8278–8300 (2012). <https://doi.org/10.3390/s120608278>
- E. Lojou, P. Bianco, Application of the electrochemical concepts and techniques to amperometric biosensor devices. *J. Electroceram.* **16**(1), 79 (2006). <https://doi.org/10.1007/s10832-006-2365-9>
- A. Margarido, in *Programa de Pós Graduação em Biotecnologia*, Desenvolvimento de biossensor baseado em microcantilever funcionalizado com biomoléculas para detecção de álcoois de cadeia curta. Development of a microcantilever based biosensor functionalized with biomolecules for the detection of short chain alcohols (Universidade Federal de São Carlos, São Carlos, 2016), p. 141. <https://repositorio.ufscar.br/handle/ufscar/8070>. Accessed 08 Nov 2021
- A. Rastegar, M. Vosgueritchian, J. Doll, J. Mallon, B. Pruitt, Nanomechanical actuation of a silicon cantilever using an Azo dye, self-assembled monolayer. *Langmuir* **29**(23), 7118 (2013). <https://doi.org/10.1021/la3034676>
- S.K. Vashist, E. Lam, S. Hrapovic, K.B. Male, J.H. Luong, Immobilization of antibodies and enzymes on 3-aminopropyltriethoxysilane-functionalized bioanalytical platforms for biosensors and diagnostics. *Chem. Rev.* **114**(21), 11083 (2014). <https://doi.org/10.1021/cr5000943>
- R. Acres, A. Ellis, J. Alvino, C. Lenahan, D. Khodakov, G. Metha, G. Andersson, Molecular structure of 3-aminopropyltriethoxysilane layers formed on silanol-terminated silicon surfaces. *J. Phys. Chem. C* **116**(10), 6289 (2012). <https://doi.org/10.1021/jp212056s>
- N.K. Chaki, K. Vijayamohan, Self-assembled monolayers as a tunable platform for biosensor applications. *Biosens. Bioelectron.* **17**(1–2), 1 (2002). [https://doi.org/10.1016/S0956-5663\(01\)00277-9](https://doi.org/10.1016/S0956-5663(01)00277-9)
- M.A. Hayat, *Principles and techniques of electron microscopy: biological applications*. vol. 3rd (Macmillan Press, London and CRC Press, Boca Raton, Florida, 1989)
- A. Margarido, B.M. Purquerio, C.R. Foschini, C.A. Fortulan, Influence of the green-machining parameters on the mechanical properties of alumina rods. *Int. J. Adv. Manuf. Technol.* **88**, 3475–3484 (2017). <https://doi.org/10.1007/s00170-016-9081-7>
- G.S. Oliveira, F.L. Leite, A.M. Amarante, E.F. Franca, R.A. Cunha, J.M. Briggs, L.C. Freitas, Molecular modeling of enzyme attachment on AFM probes. *J. Mol. Graph. Model* **45**, 128 (2013). <https://doi.org/10.1016/j.jmgm.2013.07.008>
- A.S. Maria Chong, X. Zhao, Functionalization of SBA-15 with APTES and characterization of functionalized materials. *J. Phys. Chem. B* **107**(46), 12650 (2003). <https://doi.org/10.1021/jp035877>
- T. Barr, S. Seal, Nature of the use of adventitious carbon as a binding energy standard. *J. Vac. Sci. Technol. A* **13**(3), 1239 (1995). <https://doi.org/10.1116/1.579868>
- X. Jiang, Z. Ma, J. Yu, S. Ren, H. Yang, W. Li, J. Xu, L. Xu, K. Chen, X. Huang, D. Feng, Ostwald ripening in segregated SixN/SiyN multilayers. *Phys. Status Solidi A* **213**(7), 1878–1884 (2016). <https://doi.org/10.1002/pssa.201532897>
- X. Pu, H.-B. Zhang, X. Li, C. Guia, Z.-Z. Yu, Thermally conductive and electrically insulating epoxy nanocomposites with silica-coated graphene. *RSC Adv.* **4**, 15297–15303 (2014). <https://doi.org/10.1039/C4RA00518J>

30. S. Chaudhary, T. Kamra, K.M.A. Uddin, O. Snezhkova, H.S.N. Jayawardena, M. Yan, L. Montelius, J. Schnadt, L. Ye, Controlled short-linkage assembly of functional nano-objects. *Appl. Surf. Sci.* **300**, 22–28 (2014). <https://doi.org/10.1016/j.apsusc.2014.01.174>
31. M.B. Haddada, J. Blanchard, S. Casale et al., Optimizing the immobilization of gold nanoparticles on functionalized silicon surfaces: amine- vs thiol-terminated silane. *Gold Bull.* **46**, 335–341 (2013). <https://doi.org/10.1007/s13404-013-0120-y>

Publisher's Note Springer Nature remains neutral with regard to jurisdictional claims in published maps and institutional affiliations.